Proceedings of the American Control Conference
San Diego, California • June 1999

Piezoelectric Scanners for Atomic Force Microscopes: Design of Lateral Sensors, Identification and Control [1]

A. Daniele*, S. Salapaka*, M.V. Salapaka+, and M. Dahleh*
*Department of Mechanical and Environmental Engineering, University of California, Santa Barbara, CA 93106, U.S.A.
daniele@engineering.ucsb.edu, salpax@engineering.ucsb.edu, dahleh@engineering.ucsb.edu
+Electrical Engineering Department, Ames, Iowa IA 50011, U.S.A.
murti@iastate.edu

Abstract

This paper presents the identification and control of piezoelectric positioners used in atomic force microscopes (AFM) with the goal of improving probe positioning on the sample surface. A novel sensor was developed for this task and employed to infer a sixth order linear two input two output model of the piezo's lateral dynamics. The piezo model was used to design a controller for tracking reference signals common in AFM operation. The controller and sensor were shown to significantly improve the microscope's ability to position the probe on the sample's surface, enabling the AFM user to precisely scan areas on a surface based on images from previous scans.

1 Introduction

Surfaces can be probed at the atomic level to a remarkable accuracy using the atomic force microscope (AFM). The operational idea of this tool is to detect the displacements of a microcantilever tip as the sample surface moves under it. An AFM consists of a microcantilever probe, a sample positioner, a detection system for measuring the cantilever deflections, and a control system for maintaining a desired contact force.

The sample positioners are thin-wall tubes of piezoelectric material such as PZT (lead zirconium titanate). Piezoelectric material has some undesirable properties such as hysteresis, nonlinear sensitivity, thermal drift, and creep which cause image distortions and prevent accurate repeatability. The image distortion caused by these nonlinearities can be minimized by driving the piezo with waveforms that have been carefully calibrated to produce the desired response. We will refer to this approach as the shaped waveform method. It is an open loop control method in which the controller maintains an inverse map that will undo the effects of the piezo's nonlinear sensitivity and x-y-z coupling. The drawback of this method is that the map must be corrected for changes in scan amplitude and scan speed and periodically updated as the piezo ages. *Digital Instruments* has employed this method and achieved linearity better than 1% [3].

Besides distortion free images, the ability of an AFM to position the probe repeatedly at an exact point on the sample's surface is of interest for both lithographic applications of AFM[4] and general AFM use. Experimental results shown in Figures 1 and 2 suggest that the calibrated waveform method cannot accurately reposition the probe. A 90×90 *micron* scan of an integrated circuit is made with an AFM employing the shaped waveform method (Figure 1). This large initial scan is made to identify smaller areas of interest for rescanning at higher resolutions. In this image, the user desires to rescan areas bounded by rectangles 1 and 2. The size and location of the bounding rectangles on the initial image are noted and then entered into the microscope as bias and amplitude for the second and third scans. The images resulting from scanning with these settings are shown in Figure 2c and 2e along with their respective target areas 1 and 2 enlarged and shown in 2b and 2d. Comparing these target and output images a positioning error of 20% of the target area was found.

In this paper we propose lateral feedback as an alternative solution for correcting image distortion and as a means of improving the repeatability of scans. We show that images of similar quality can be achieved with better repeatability than with the shaped waveform method. The closed loop solution requires sensors to be added to the AFM for measuring the lateral piezo movement. For this purpose we have developed optically based sensors and integrated them into a *Digital Instruments Multi-Mode AFM* by replacing the manufacturer's scanner with one fabricated at UC Santa Barbara. The sensors enabled us to develop a linear two input two output non-parametric model G of the piezo positioner's lateral dynamics. The model

[1]Research supported by NSF under Grant ECS-9632820 and ECS-9733802, URG Grant # 7041721 by ISU, and AFOSR under Grant F49620-97-1-0168.

was used to design a diagonal controller K with loop shaping techniques. The controller was discretized and implemented in a feedback loop with the sensors. It was demonstrated by using feedback control that performance gains were made in scan repeatability.

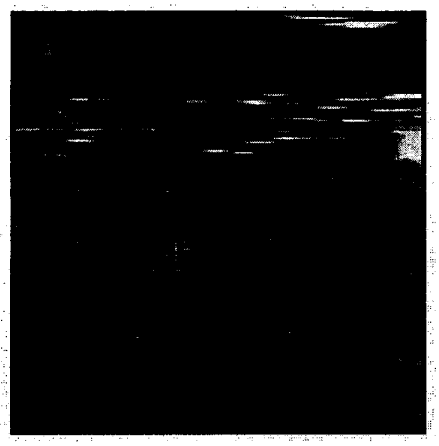

Figure 1: A large 90 x 90 *micron* scan of an IC using made by AFM with open loop control in x and y. Black rectangles 1 and 2 are defined by user for rescanning at higher spacial. The bais and amplitude corresponding to rectangles location and size are entered into the microscope. The resulting scans are shown in Figure 2.

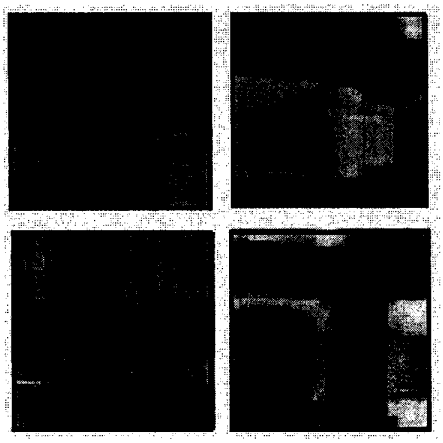

Figure 2: Images B and D are target areas 1 and 2 defined in Figure 1. Images C and E are output scans while x and y controlled open loop.

2 Sensor

Several methods have been proposed to measure the lateral displacements of piezoelectric tubes, which include capacitive, interference, and strain based techniques [8]. We employ a design based on optical levers,

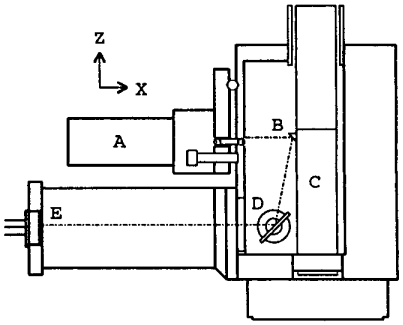

Figure 3: Cross-section of the UCSB scanner showing piezo positioner and lateral sensor for detection of the piezo motion in the x direction.

similar in principle to the detection system used to measure deflections in the cantilever probes. In the detection scheme, a collimated laser marked (A) in Figure 3 shines on a small mirror (B) attached to sidewall of piezo tube (C). The light is reflected downward to a swivel mirror (D) and directed to a pair of closely spaced photodetectors (E). Deflections of the tube cause one photodetector to collect more light than the other, and the output of the differential amplifier, which is proportional to the deflection of the piezo, is used to measure the lateral travel. The sensor setup shown in Figure 3 is duplicated for measurement of piezo movement in the y direction.

The sensors were calibrated using a calibration reference sample with known feature size. The resolution of the sensor was noise limited and taken as 4σ, where σ is the standard deviation of noise amplitude. We operated the sensor in the region in which the response was linear. The drift of the sensor was measured by recording the sensor's output for one hour with the piezo undriven. The following table presents some performance measures of the sensor.

	x direction		y direction	
sensitivity	3.61	$\mu m/V$	4.52	$\mu m/V$
bandwidth	90	Hz	90	Hz
noise level	20	nm	20	nm
drift	1.65	$\mu m/hr$	0.63	$\mu m/hr$
linearity	0.7	%	1.2	%
range	40	μm	40	μm

3 Identification

The desired closed loop system is shown in Figure 4. Let G be the model of piezo scanner, S be the sensor model , and K be the controller. G maps applied voltage $u = \{u_1, u_2\}^T$ to sample displacement $w = \{w_1, w_2\}^T$, where subscripts 1, 2 denote the x, y di-

rections respectively. G is then a 2×2 transfer-function matrix, whose elements G_{ij} are scalar transfer functions from j^{th} element of u to i^{th} element of w. Model G neglects the non-linear behavior of piezo but was found sufficient for the design of the controller. The sensor S is also a 2×2 transfer-function matrix from sample displacement w to sensor voltage $y = \{y_1, y_2\}^T$. A model of S can be obtained from the capacitor and resistor values in the filters present in the sensors. The photodiode gain from the piezo displacement to voltage is 3.614 $\mu/volt$ and 4.523 $\mu/volt$ for the x and y directions. We assumed S to be diagonal and attributed all coupling in the system to G. The model used for S is

$$S(s) = diag\{S_1(s), S_2(s)\}, \quad (1)$$

where,

$$S_{1,2}(s) = \frac{k_{1,2}}{(a_1 s + 1)(a_2 s + 1)} \quad (2)$$

with $a_1^{-1} = 556\ rad/sec$, $a_2^{-1} = 611\ rad/sec$, $k_1 = 3.614\ \mu m/volt$, and $k_2 = 4.523\ \mu m/volt$.

We employed a nonparametric method of system identification [1],[2] to obtain our model G. We cannot measure the displacement of the piezo and therefore can not directly obtain the frequency response of elements G_{ij}, so we introduce sensors S which transduce displacement w in *microns* into a measurable signal y in *volts*. The measurements are then made of the cascade SG, from which we extract the response of G. This is done by measuring the response of each cascade element $[SG]_{ij}$, then multiplying the response by the simulated frequency response of S_i^{-1}, which gives the frequency response of G_{ij} alone. Note that,

$$[SG] = \begin{bmatrix} S_1 G_{11} & S_1 G_{12} \\ S_2 G_{21} & S_2 G_{22} \end{bmatrix} \quad (3)$$

$$G_{ij}(j\omega) = S_i^{-1}(j\omega)\,[SG]_{ij}(j\omega). \quad (4)$$

The measurements after deconvoluting the sensor effects are shown in Figure 5 as solid lines. To arrive at our model G, a twelfth order rational function was fit to each of the four frequency response data sets using MATLAB tools. This results in four twelfth order single input single output (SISO) models, one for each of the four subsystems of G. The models were then combined into a forty-eighth order state-space model. The model was balanced and then reduced by setting the derivative of states $7 \ldots 48$ equal to zero and solving for the remaining states. The frequency response of the resulting sixth order model G is plotted in Figure 5 with dotted lines. The plots show that the first resonance of the G_{11} and G_{22} elements are captured by the model, as well as the first two resonances of the G_{12} and G_{21} elements. The model of G_{12} is non-minimum

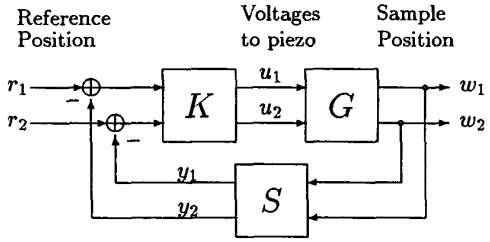

Figure 4: Block diagram of the closed loop system. The controller is marked K, piezo G, and lateral sensor S.

phase, but inspection of the measured frequency response suggest that this is an artifact of the fit, rather than property of the piezo system.

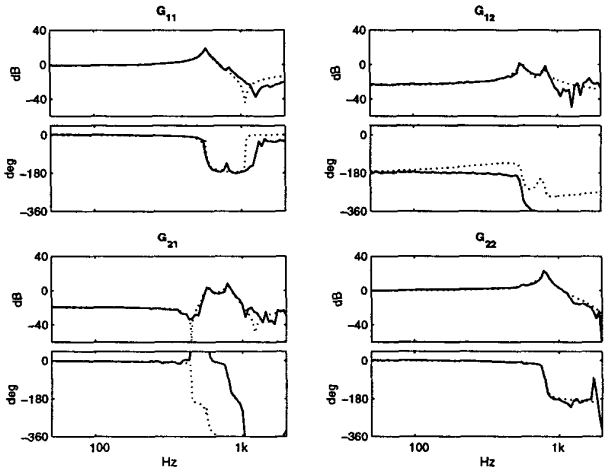

Figure 5: Measured frequency response of G after deconvoluting sensor effects (solid) and response of sixth order MIMO model of G (dotted).

4 Control Design

For the design of controller K we employ the loop-shaping procedure that involves explicitly shaping the open loop transfer function $L = SGK$. For this design we neglect the coupling terms in piezo model G, reducing it to a diagonal matrix $G_d = diag\{G_{11}, G_{22}\}$. Assuming the G_d plant, our problem of finding a multi-input multi-output controller is recast as the design of controllers for two single input single output plants, G_{11} and G_{22}.

The reference signals to track for this problem are

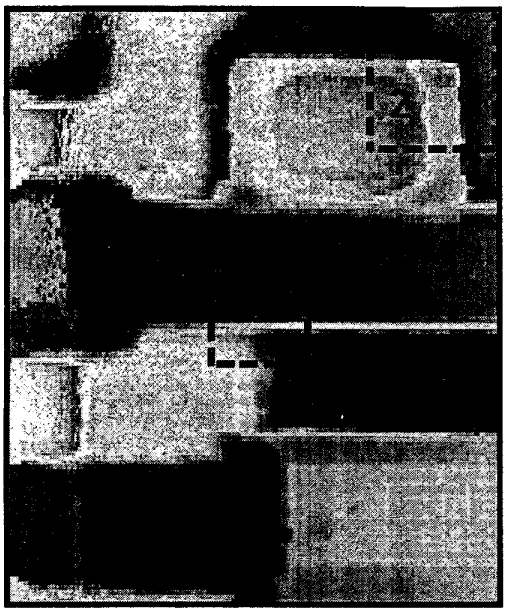

Figure 6: A 40 × 40 *micron* scan of integrated circuit while probe's x and y movements were controlled with feedback. Target areas 1 and 2 were defined by user for high resolution rescanning. The location and size of the dashed boxes were used to form the reference signal for rescans shown in Figure 7.

based on the desired movement of the probe across the sample's surface. The path of the probe while scanning is a raster pattern in which the probe repeatedly traces lines on the surface in the x direction while slowly increasing its position in the y direction. A grid of measurement points on the sample's surface is obtained by sampling this path at a constant time interval. The reference signals r for this pattern are $0.25Hz$ to $4Hz$ triangle waves in x direction and a $31.2mHz$ to $2mHz$ ramp in y direction. These ramps have laplace transform $1/s^2$, requiring a $1/s^2$ term to appear in L for perfect tracking. The $1/s^2$ term is not present in S or G_d, so it is included in the controller K. To counter the loss of phase due to the $1/s^2$ term in K, we place a zero in K prior to the crossover frequency[1] ω_c. This zero will add phase to L near ω_c, giving a better phase margin. At high frequencies L should roll off to attenuate noise and provide robustness. Rather than adding additional poles to K after w_c we rely on the sensor poles in S to attenuate L at high frequency. A controller K that satisfies these conditions has the form

$$K(s) = diag\{K_1(s), K_2(s)\}, \quad (5)$$

[1] crossover frequency is the frequency ω at which $|L(j\omega)| = 1$.

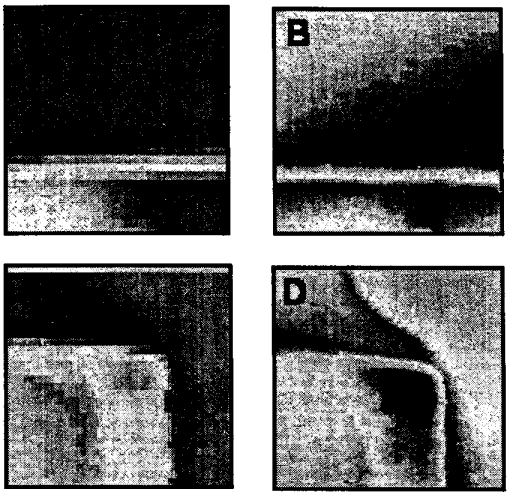

Figure 7: Figures A and C are the enlargements of the target areas 1 and 2 shown in Figure 6. Images B and D are rescans of areas 1 and 2 with x and y directions controlled with feedback.

where,

$$K_{1,2}(s) = k\frac{b\,s+1}{(a\,s+1)^2}. \quad (6)$$

The $1/s^2$ term was approximated with $1/(a\,s+1)^2$ where a is large. This was done so that the controller is stable, a desirable property in an experimental setting. After a few iterations the values were selected as $a^{-1} = 2\pi\ rad/sec$, $b^{-1} = 30\pi\ rad/sec$, and $k = 540$. The same values are taken for K_1 and K_2 due to the similarity between the G_{11} and G_{22} frequency responses. K was discretized using *zeroth-order hold* method [7] and implemented on a DSP board. The controller K and sensor S were placed in a feedback loop with G and the closed loop frequency response from r to y measured. Close agreement between simulated and measured responses was found.

Performance of the closed and open loop systems in the time domain were compared by having the systems track a $4Hz$ triangle wave in the x direction and a constant setpoint in the y direction. Performance is quantified by the sum of the distance error of the probe from the intended path over a single period of the reference. That is,

$$|e| = \sum_t dist(r,y)(t) \quad (7)$$

where $dist(p,q)(t)$ is the Euclidean distance between points p and q at time t.

For comparison we measure the open loop response of the system by letting $u = r$ and recording y. The response for the x direction is shown at the top of Figure 8. The loop was then closed as in Figure 4 and the x direction response output measured again. The results are shown in the bottom of Figure 8. Tracking error $|e|$ was calculated for both configurations and a reduction by 73% in the tracking error was found by employing feedback. Comparing Figures 8a and 8c we see that piezo tracks the triangle wave reference more closely with feedback. From Figure 8b and 8d, we also see that the peak overshoot is reduced from 9% of the primary channel displacement to 1.8% by employing feedback.

5 Closed Loop Scanning

The closed loop performance was evaluated by conducting an experiment similar to the one discussed in the introduction of this paper. A 40×40 *micron* scan of an integrated circuit with low spactial resolution was made. The piezo was made to track the desired raster pattern using feedback control. The image is shown in Figure 6. The image was inspected and two regions of interest were identified on the image and bounded with rectangles 1 and 2. The location and size of the rectangle on the low resolution image were used to form the reference bias and amplitude for the second and third scans. The probe then scanned over these areas while being controlled with feedback in the x and y directions. The rescanned images are shown in 7b and 7d along with the target areas 1 and 2 in 7a and 7c. A comparision of 7a,c and 7b,d shows that the closed loop system can scan with a higher degree of repeatablity than the open loop system shown in 2b,c and 2d,e.

6 Conclusions

In this paper we have proposed lateral feedback as a solution for correcting image distortions in AFM and as a method of improving probe placement on the sample's surface. Using lateral sensors and non-parametric identification techniques, we were able to describe the piezo positioner lateral motion with a low order LTI MIMO model that was sufficient for linear control design. Loop shaping techniques were employed for designing controller to track common AFM signals. The closed loop system was implemented on AFM and it was shown that accurate positioning with a higher degree of repeatiblity is achievable with lateral feedback.

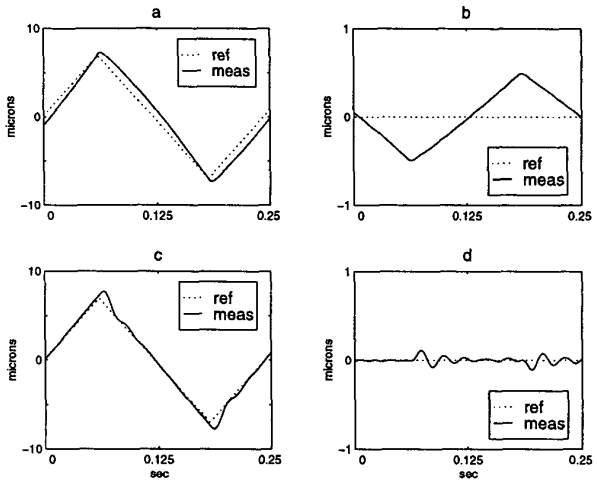

Figure 8: Figure show open and closed loop systems tracking $4Hz$ triangle wave in x direction and constant setpoint in y direction. Top left and top right are measured x and y displacement for the open loop system. Bottom left and bottom right are measured x and y displacement for closed loop system.

References

[1] L. Ljung, System Identification Theory For The User *P T R Prentice Hall Information and System Sciences Series.*

[2] T. Soderstrom and P. Stoica, System Identification, *Prentice Hall.*

[3] MultiMode Scanning Probe Microscope Instruction Manual *Digital Instruments, Santa Barbara, California* MN-REF-COM-4.31ce, Rev.A-20AUG97.

[4] J.A. Dagata and C. Marrian, Technology of Proximal Probe Lithography, *SPIE Optical Engineering Press* Volume IS 10, 1993.

[5] C. W. deSilva, Control Sensors and Actuator, *Prentice Hall 1989,Englewood Cliffs, New Jersey.*

[6] S. Skogestad and I. Postlethwaite, Multivariable Feedback Control, Analysis and Design, *John Wiley and Sons.*

[7] Gene F. Franklin and J. David Powell, Digital Control of Dynamic Systems, *Addison-Wesley Publishing Company.*

[8] E. Meyer, Atomic Force Microscopy, *Surface Science*, Vol.41,p3-49,1992

[9] E. O. Doebelin, Measurement Systems, *McGraw-Hill Book Company.*